

# Synthesis of the Nanostructured Zinc Oxide Using the Soft template of *Cylea barbata* Miers Extract and its Promising Property for Dye Adsorbent

O. Zuas<sup>a,\*</sup>, A. Kristiani<sup>a</sup>, A. Haryono<sup>a</sup>

<sup>a</sup> *Research Centre for Chemistry-Indonesian Institute of Sciences (RCChem-LIPI), Kawasan PUSPIPTEK Serpong 15314, Tangerang, Indonesia.*

---

## ARTICLE INFO

### Article history:

Received 23 November 2014

Accepted 07 January 2015

Available online 15 March 2015

### Keywords:

Zinc oxide

Nanostructure

*Cylea barbata*

Soft-template

Adsorbent

---

## ABSTRACT

Nanostructured zinc oxide (ZnO) was successfully synthesized by precipitation method using the extract of *Cylea barbata* Miers (CBM) leaves as a soft template after 3 h of calcinations in furnace at 500°C in the open air. Characterization results showed that the nanostructured ZnO had hexagonal wurtzite structure with space group P63mc and nano-scale particle diameter. It was suggested that the existence of polysaccharide galacturonic acid as the major bio-molecular component in the CBM extract induced the formation of the nanostructured ZnO. Preliminary study results through activity testing of adsorption for Congo red (CR) dye removal from aqueous solution showed that the nanostructured ZnO exhibited excellent adsorption property, indicating that its adsorption activity was better than that of the commercial ZnO. Regeneration study of the nanostructured ZnO indicated that it could be reused while its adsorption activity was kept excellent with removal efficiency > 85% even up to five times of the cycling experiments.

---

## 1. Introduction

As a semiconductor material, nanostructured zinc oxide (ZnO) has attracted considerable interest in both academic and research institutes because it exhibits tremendous physical and chemical properties, which are significantly different from the ZnO bulk particles. As a versatile semiconductor the nanostructured ZnO has been used as a material for solar cell [1], semiconductor device [2], environmental remediation [3], and biomedical treatment [4]. In solar cell application, ZnO was found to increase the performance of hybrid solar cell device [1]. For semiconductor device application, it has been used for the synthesis of

ultraviolet photodiode based on ZnO nano-wire [2]. It has also been reported as an active material for remediation purposes, including heavy metal and toxic dyes removal from aquatic environment [3, 5]. In the biomedical application, the efficiency of the nanostructured ZnO has been reported as an anti-microbial agent to treat pathogenic bacteria [4, 6].

To date, a number of methods for the synthesis of nanostructured ZnO, including microwave-assisted [7], sol-gel [8], ultrasonication [9], solvo/hydrothermal [10], surfactant-assisted [11], sonochemical [12] and electrochemical deposition [13], have been reported. Among these methods, surfactant-assisted

---

Corresponding author:

E-mail address: oman.zuas@lipi.go.id (Oman Zuas).

method is preferred because of its simplicity. Further, the surfactant used as the capping agents in this method can suppress the particle growth, so nano size of ZnO particle can be achieved. The employed templates in the above process may include cetyltrimethyl ammonium bromide [14], polyethylene glycol [15, 16], polyvinyl pyrrolidone [17], poly acrylic acid [18], and sodium dodecyl sulfate [19]. However, surfactant-based templates suffer from several disadvantages, including high price, poor mechanical strength, and time-consuming template removal. Recently, the use of bio-template resourced from nature including albumen [20], cotton fibers [21], gelatin [22], palm olein [23], microbial cells [24], rice [25], and virus [26] for the synthesis of nanostructured ZnO has been reported and emerged as an alternative to the conventional methods. The specific advantages of this bio-inspired method in comparison with the conventional surfactant-assisted ones include: i) it involves an inexpensive route because the bio-template can be easily obtained from an abundant resource in nature while keeping the process to be green and environmentally friendly; ii) it generates the nanostructured ZnO with improved mechanical properties; iii) it can be easily scaled up for a large production scale. Despite the fact that the usage of several resources in nature for the synthesis of nanostructured ZnO has been pointedly achieved, exploring other bio-inspired templates in the area is still facing challenges. It is a widely acceptable idea that synthesis of metal oxide is generally designed to achieve an active material that is otherwise not reactive [27]. Thus, the purpose of this study is not only to synthesize the nanostructured ZnO but also to evaluate its activity. In general, colored synthetic dyes are commonly used in many industries such as cotton textile, plastic, wood pulp and paper. The occurrence of colored dye in aquatic environment is most closely related to the improper method used for discharging of the industrial effluents. The presence of colored dye effluents can potentially threaten the aquatic ecosystem because they are aesthetic pollutants, resistant to aerobic digestion, stable to both light heat and oxidizing agents, and they can hinder the light penetration required

for the aqueous biological processes [28, 29]. In addition, the colored effluents may contain some harmful chemicals that are toxic, carcinogenic, or mutagenic to aquatic life [28-30]. Here, we report a work on the synthesis of nanostructured ZnO using an aqueous extract of *Cyclea barbata* Miers (hereafter abbreviated as CBM) leaves as bio-template. The synthesized nanostructured ZnO was then characterized using thermogravimetric analyzer (TGA), X-ray diffraction (XRD) analysis, Fourier transform infrared (FTIR) spectroscopy, Brunauer-Emmett-Teller (BET) surface analysis, and scanning electron microscopy (SEM). The activity of the nanostructured ZnO as adsorbent for removal of dye wastewater pollutant was evaluated with Congo red (CR) as the colored dye model.

## 2. Experimental

### 2.1. Materials

Commercially available chemicals were used without further purification. The chemicals include ammonia solution (NH<sub>4</sub>OH, 25%, Merck, Germany), zinc acetate dihydrate (Zn(CH<sub>3</sub>COO)<sub>2</sub>·2H<sub>2</sub>O, 98%, Merck, Germany), Congo red dye (C.I. 22120, 97% Sigma-Aldrich, Germany) having a molecular structure as presented in Fig. 1a. Fresh CBM leaves (Fig. 1b) were collected from a farm in Kota Tangerang, Banten, Indonesia. Deionized water was used in all experimental runs.

### 2.2. Experimental Design

#### 2.2.1. Preparation of the CBM leaves extract

The CBM leaves extract used in this study was prepared through the following simple procedure. Typically, fresh CBM leaves were thoroughly washed twice with 200 mL of deionized water in order to remove the dust particles. 5 g of free-dust CBM leaves was then transferred into a household blender containing 150 mL of deionized water. After 30 seconds of blending, the blended CBM leaves were sieved through a 106 mesh wire net to obtain the CBM aqueous extract for further immediate use.

#### 2.2.2. Synthesis of the nanostructured ZnO

The nanostructured ZnO was synthesized by a

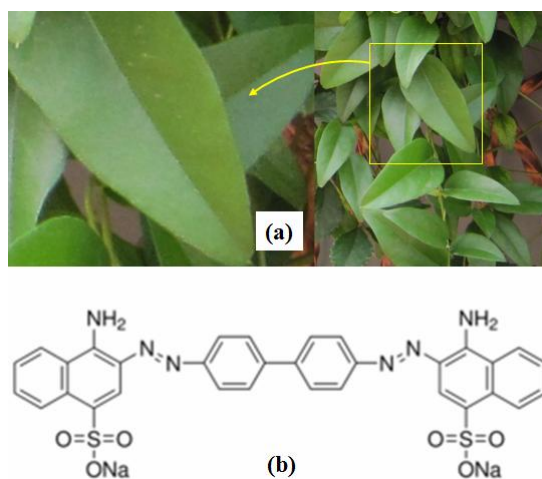


**Fig. 1.** *Cyclea barbata*, Miars leaves (a), and the molecular structure of CR dye (b). (For interpretation of the references to color in this figure the reader is referred to the web version of the article.)

simple precipitation method using the leaf extract of CBM as a bio-template with  $\text{NH}_4\text{OH}$  as a precipitating agent. In a typical procedure, 4.45 g of  $\text{Zn}(\text{CH}_3\text{COO})_2 \cdot 2\text{H}_2\text{O}$  was dissolved in 100 mL of the CBM leaves extract in a 250 mL beaker glass under vigorous stirring to obtain a mixture solution containing the CBM leaves extract and  $\text{Zn}(\text{CH}_3\text{COO})_2 \cdot 2\text{H}_2\text{O}$ , giving solution I. After stirring for 10 min,  $\text{Zn}(\text{CH}_3\text{COO})_2 \cdot 2\text{H}_2\text{O}$  in solution I was slowly precipitated using the  $\text{NH}_4\text{OH}$  solution (25% v/v) until the pH of the solution reached the value of 10, giving solution II. This solution was continuously stirred for 10 min, followed by incubating in an oven at  $65^\circ\text{C}$  for 18 h. After incubation, the liquid of solution II was discarded by centrifugation at 2200 rpm for 5 min to obtain the CBM gel containing zinc hydroxides [CBM-Zn  $(\text{OH})_2$  gel]. The CBM-Zn  $(\text{OH})_2$  gel was washed three times with deionized water followed by washing with 50 mL of ethanol. The washed CBM-Zn  $(\text{OH})_2$  gel was dried in an oven at  $105^\circ\text{C}$  for 2.5 h and then at  $120^\circ\text{C}$  for 1 h to produce the precursor of nanostructured ZnO (the as-prepared synthesized sample). Finally, nanostructured ZnO was obtained by calcining the as-prepared synthesized sample at  $500^\circ\text{C}$  for 3 h.

### 2. 2. 3. Characterization

Thermal gravimetric analysis (TGA) of the as-prepared synthesized sample was carried out on a Mettler-Toledo TGA 851e. The sample was placed in an alumina crucible and heated in

the temperature ranging from 25 to  $700^\circ\text{C}$  at a heating rate of  $5^\circ\text{C}/\text{min}$  under a nitrogen atmosphere. For the synthesized nanostructured ZnO, the XRD data were recorded on a Rigaku X-ray at 40 kV and 100 mA with  $\text{Cu-K}\alpha$  as the radiation source. The  $2\theta$  was scanned in the range from  $25^\circ$  to  $75^\circ$  at a speed of  $1.2^\circ/\text{min}$ . The FTIR spectra of all samples under investigation were recorded on a Shimadzu IR Prestige DSR-8000 spectrometer using potassium bromide (KBr) media in the wavenumber ranging from  $400\text{ cm}^{-1}$  to  $4000\text{ cm}^{-1}$  at a scanning rate of  $4\text{ cm}^{-1}/\text{min}$ . The specific surface area of the synthesized nanocomposite samples was determined using a multi-points BET method from the  $\text{N}_2$  adsorption-desorption isotherm on a Quantasorb sorption system-Quantachrome Corporation surface area analyzer. Before the BET analysis, the nanostructured ZnO sample was dried at  $120^\circ\text{C}$  overnight and then out-gassed at  $300^\circ\text{C}$  for 3 h. Morphological analysis of the synthesized nanostructured ZnO was conducted on a JEOL SEM (JSM-6400V) operated at 20 KV with gold sputtered on sample. The TEM image of the synthesized nanostructured ZnO was recorded on a TEM-2100F high resolution TEM operating at 200 kV. The nanostructured ZnO for TEM analysis was dispersed in ethanol, sonicated and then one drop of the suspensions was deposited onto a 300 mesh copper grid.

### 2. 2. 4. Dye adsorption evaluation

Adsorption studies of the CR dye by

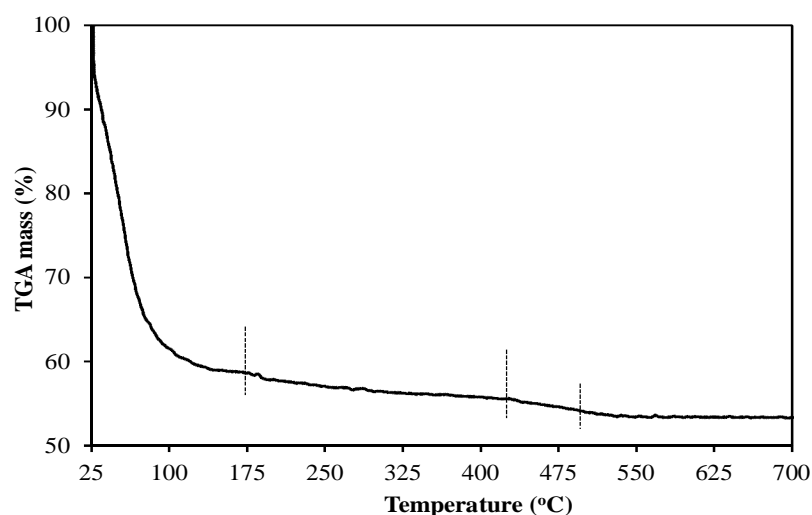


Fig. 2. The TGA thermograph of the as-prepared synthesized sample.

nanostructured ZnO were conducted using batch experimental methods. In general, a certain amount (mg) of nanostructured ZnO was transferred into a 15 mL capped glass tube containing 10 mL of the CR dye solution. The tube was then placed in a Cetromat WR temperature-controlled water bath shaker and agitated for a certain duration under specified conditions (130 rpm and  $30 \pm 1^\circ\text{C}$ ). Afterward, supernatant solution was separated from the adsorbent by centrifugation at 2200 for 5 min using IEC Centra CL2 Thermo centrifuge. In order to determine the residue of the CR dye in the solution, the absorbance of supernatant solution was measured at maximum wavelength ( $\lambda_{\text{maks}}$ ): 500 nm using Hitachi U-2000 UV-Vis spectrophotometer. The concentration of the CR dye remaining in the solution was calculated by inserting the absorbance of individual sample solutions into a calibration curve expression, which was obtained by plotting the CR dye standard solutions versus their concentration. A high linearity of the calibration curve was obtained by measuring a series of the CR dye standard solution ranging from 2.5-10 mg/L, giving an expression:  $A = 0.0355C - 0.0036$ , where A and C are the absorbance and concentration of the CR dye standard solutions, respectively. The coefficient regression ( $R^2$ ) of the calibration curve expression was found to be 0.9988. The percentage removal (%R) of the CR dye was calculated using the following expression:

$$\%R = \frac{(C_o - C_t)}{C_t} \times 100 \quad [1]$$

where  $C_o$  (mg/L) is the initial concentration of the CR dye solution and  $C_t$  is the concentration of CR dye after time t (mg/L).

### 3. Result and discussion

#### 3. 1. Characterization of the nanostructured ZnO

Thermal gravimetric analysis (TGA) technique is commonly used to investigate mass loss of the heat treated materials as a function of increasing temperature. Fig. 2 shows the TGA thermograph of the as-prepared synthesized sample. As can be seen in Fig. 2, the first broad TGA exothermic peak was observed in the temperature range of 25-175 oC, which may indicate the mass loss due to the evaporation of the surface adsorbed water [31], attributing to a mass loss of 41.35%. The second TGA exothermic peak was observed at the temperature range of 175-425oC, indicating the mass loss caused by the decomposition of hydroxyl groups and organic molecules chemically bonded to the material surface [32]. This peak occurred with a mass loss of 3.07%. The last TGA exothermic peak was found in the temperature range of 425-500°C, giving a mass loss of 1.58%. A small decreasing of the material mass can be assumed due to the change of the ZnO phase from amorphous to crystalline phase. From the TGA thermograph

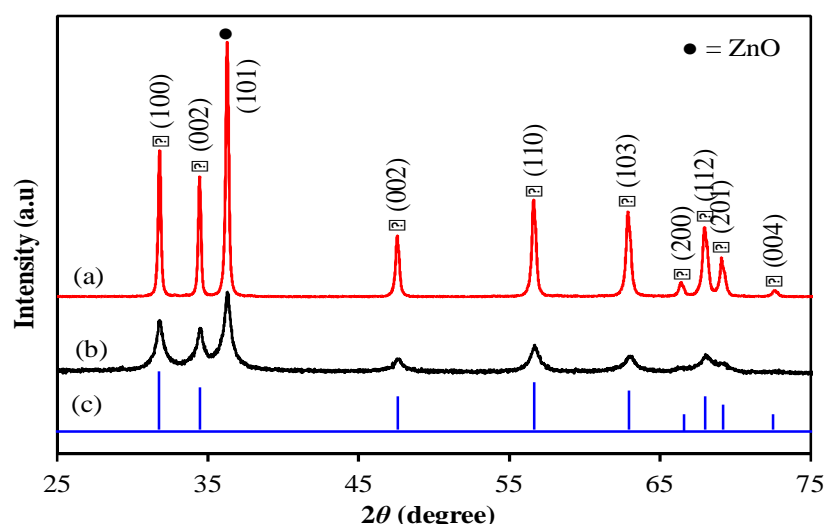


**Fig. 3.** The XRD pattern of the commercial ZnO (a), the synthesized nanostructured ZnO calcined at 500 oC (b), and the XRD pattern of the ZnO according to the JCPDS Card No 36-1451(c). (For interpretation of the references to color in this figure the reader is referred to the web version of the article.)

data it can be concluded that the suitable temperature for calcination of the as-prepared synthesized sample to obtain nanostructured ZnO is 500°C.

Fig. 3 shows the XRD pattern of the sample under this study. Fig.3a shows the XRD pattern of the commercial ZnO, which is included for comparison only. As can be seen from Fig. 3a, the XRD of the commercial ZnO has well-defined diffraction peaks at about 31.81°, 34.45°, 36.29°, 47.57°, 56.63°, 62.89°, 66.43°, 67.95°, 69.07°, and 72.69°. These diffraction peaks are assigned to (100), (002), (101), (102), (110), (103), (200), (112), (201), and (004) planes, respectively. Very similar XRD peak pattern was observed for the nanostructured ZnO (Fig. 3b), although its peak height was found to be lower than the commercial ZnO. Interestingly, all of the diffraction peaks in both commercial and synthesized nanostructured ZnO can be indexed to the hexagonal wurtzite structure with space group of P63mc by comparison with the data from JCPDS Card No. 36-1451 as shown in Fig. 3c [33]. No diffraction peaks arising from any impurity can be detected in the pattern, which confirms that the grown products are pure ZnO. Fig. 4a, 4b and 4c show the FT-IR spectra of the as-prepared synthesized sample, the nanostructured ZnO, and the commercial ZnO, respectively. From Fig. 4a, it can be seen that

the FTIR of the as-synthesized sample shows some characteristic peaks of polysaccharides in the form of polygalacturonic acid as the main component of the CBM extract [34]. The bands at around 2930 cm<sup>-1</sup> indicate the presence of the O-CH<sub>3</sub> stretching from methyl esters. The absorption band around 1760-1745 cm<sup>-1</sup> is assigned to the ester group, while the band at around 1640-1620 cm<sup>-1</sup> is attributed to the free carboxylic groups (1640-1620 cm<sup>-1</sup>) [35]. The O-H (νO-H) bending vibration of the physisorbed water is observed with the peak at around 3400 cm<sup>-1</sup> [27]. All these bands almost disappear in the FT-IR spectrum of the nanostructured ZnO after calcination at 500°C for 3 h (Fig. 4b), indicating the polysaccharides component has been eliminated during calcination. In addition, some typical bands of the ZnO can be observed in Fig. 4b. A stretching vibration mode of Zn-O (νZn-O) in the nanostructured ZnO is observed at about 430 cm<sup>-1</sup>. The peak at around 1064 cm<sup>-1</sup> might be attributed to C=C stretching mode. The peak of the C-O bond is observed at around 1706 cm<sup>-1</sup>. The broad band at around 3340 cm<sup>-1</sup> is assigned to the existence of hydroxyl group (-OH) on the surface of the sample. The peak at around 2480 cm<sup>-1</sup> indicates the existence of CO<sub>2</sub> molecules in air. Those bands at around 2800-3000 cm<sup>-1</sup> are due to the C-H stretching frequencies [36, 37]. Moreover,

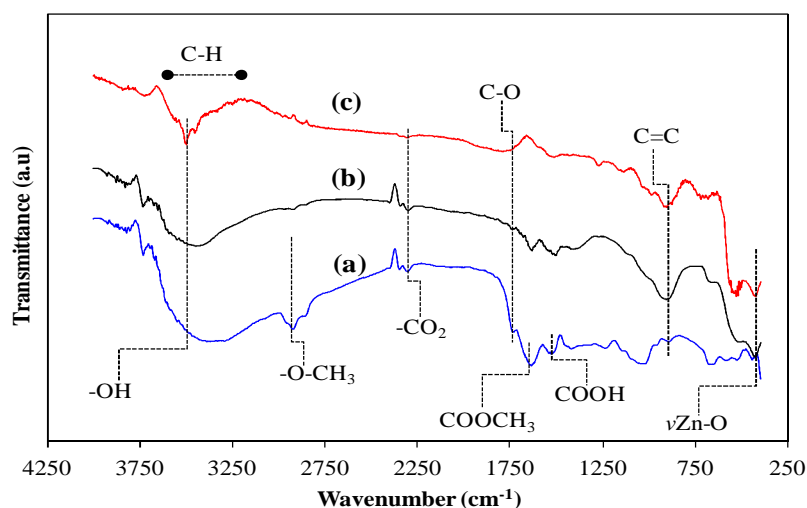


**Fig. 4.** The FT-IR spectra of the as-prepared synthesized sample (a), the nanostructured ZnO calcined at 500 °C for 3 h (b), and of the commercial ZnO (c). The commercial ZnO is included for comparison only. (For interpretation of the references to color in this figure the reader is referred to the web version of the article.)

the FT-IR spectrum of the nanostructured ZnO (Fig. 4b) has a pattern similar to pure commercial ZnO (Fig. 4c). This finding is an agreement with the XRD data, ensuring that the synthesized material obtained is ZnO.

The typical nitrogen adsorption–desorption isotherm of nanostructured ZnO and its corresponding pore-size distributions are shown in Fig. 5a and 5b, respectively. As shown in Fig. 5(a), the adsorption–desorption isotherm of nanostructured ZnO is identified as type IV, showing a mesoporous material characteristic [38]. The BET surface area of nanostructured ZnO is about 54 m<sup>2</sup>/g, which is obviously larger than that of commercial ZnO powder with a BET surface area of about 3.3 m<sup>2</sup>/g [39]. The BJH pore-size distribution ranges from 13 nm to 75 nm with an obvious maximum at about 42 nm. Conclusively, all these data indicates that the nanostructured ZnO may have strong adsorption behavior. The SEM image of the nanostructured ZnO showed that the ZnO particles were almost spherical in shape (Fig. 6). From the high resolution TEM image of the nanostructured ZnO particle (inset of Fig. 6), the grain boundary of the nanostructured ZnO can be clearly observed with a clear crystal diameter of about 10-20 nm, which is smaller than the commercial ZnO with average particle size of about 500 nm [39]. As can be seen from the image (inset of

Fig. 6), most of the particles' shapes consist of several spheres attaching together. The main component of CBM is polygalacturonic acid, which is a polysaccharide compound. It has been previously reported that polysaccharide can play an important role when they are used in the synthesis of metal oxide based materials, because they can act as capping, functionalizing, stabilizing, poring and/or coordinating agents [25]. Besides, the hydroxyl groups of the polysaccharides might be involved in intra- and/or intermolecular supramolecular association or might be coordinated with transition metal ions, preserving the particle highly aggregated [40]. Moreover, this template-assisted method is considered as a soft-templating method since CBM was used to synthesize mesoporous ZnO nanostructures. Based on the discussion above, a possible mechanism for the formation of the nanostructured ZnO may be suggested as shown in Fig. 7 and the description is as follows. The self-assembly of the CBM extract and organization of zinc ion over the CBM extract formed a solid and stable inorganic-organic hybrid (Fig. 7a). The addition of NH<sub>4</sub>OH leads to formation of the Zn(OH)<sub>2</sub>-CBM extract and NH<sub>4</sub>(CH<sub>3</sub>COO) aqueous solution (Fig. 7b). The removal of the NH<sub>4</sub>(CH<sub>3</sub>COO) aqueous solution yields wet solid CBM-Zn(OH)<sub>2</sub> gel

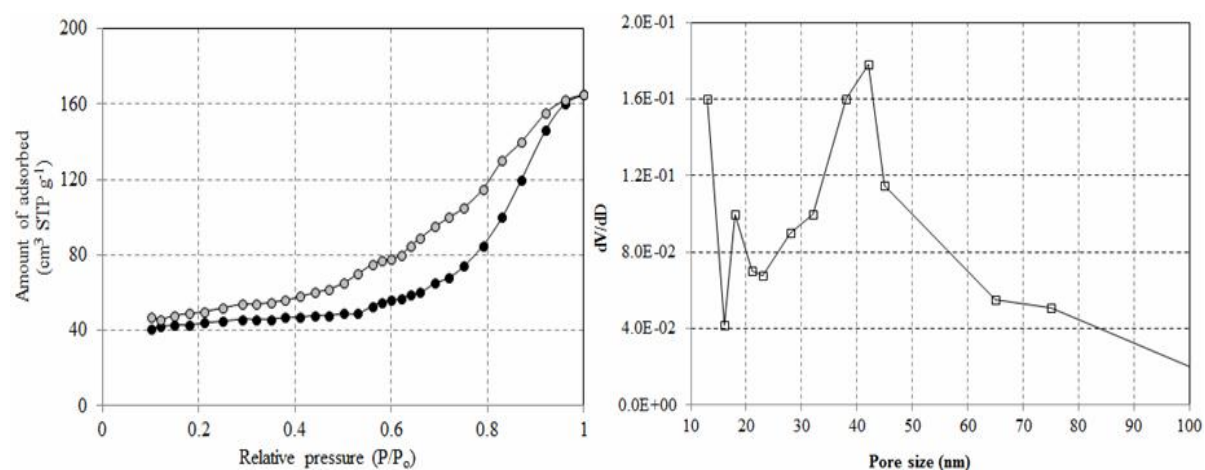


**Fig. 5.** Nitrogen adsorption-desorption isotherm for the nanostructured ZnO (a), and pore size distribution plot (b).

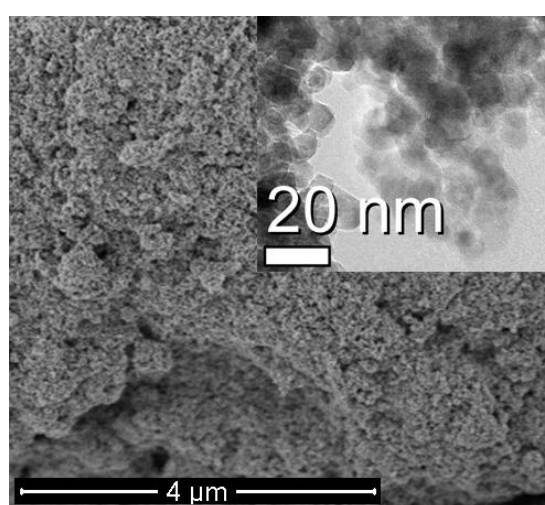


**Fig. 6.** SEM image of the nanostructured ZnO calcined at 500 °C for 3 h (Inset: TEM image)

(Fig. 7c). The drying of wet solid CBM-Zn(OH)<sub>2</sub> gel produced dry solid CBM-Zn(OH)<sub>2</sub> (Fig. 7d). The removal of the CBM template by the calcination of dry solid CBM-Zn(OH)<sub>2</sub> at 500 °C for 3 h produced phase-pure nanostructured ZnO (Fig. 7e).

### 3. 2. Adsorption Testing for CR Removal

A simple re-calculation allows to plot the percentage removal as the functions of contact time (Fig. 8a). It was shown that adsorption increases rapidly in the initial stages. This rapid adsorption process might be due to rapid attachment of the CR dye to the surface of the nanostructured ZnO. Increasing of the adsorption is kept gradual until equilibrium is reached and then remains constant. It can be observed that the remaining percentage

removal becomes asymptotic to the time axis after 90 min of shaking. Moreover, the amount of the CR dye adsorbed showed no significant difference when the contact times were longer than 100 min. This duration, i.e. 100 min, was found to be sufficient for reaching the adsorption equilibrium of the CR dye.

In addition, the synthesized nanostructured ZnO was compared to a commercial ZnO powder for their removal efficiency. It was found that the removal efficiency of the nanostructured ZnO was 58.49 %, which was higher than that of the commercial ZnO (Fig. 8b). Normally, some good adsorbent can be used several times after regeneration by removing the adsorbate from the surface of adsorbent. Hence, regeneration of the used adsorbent is essential. However, incomplete

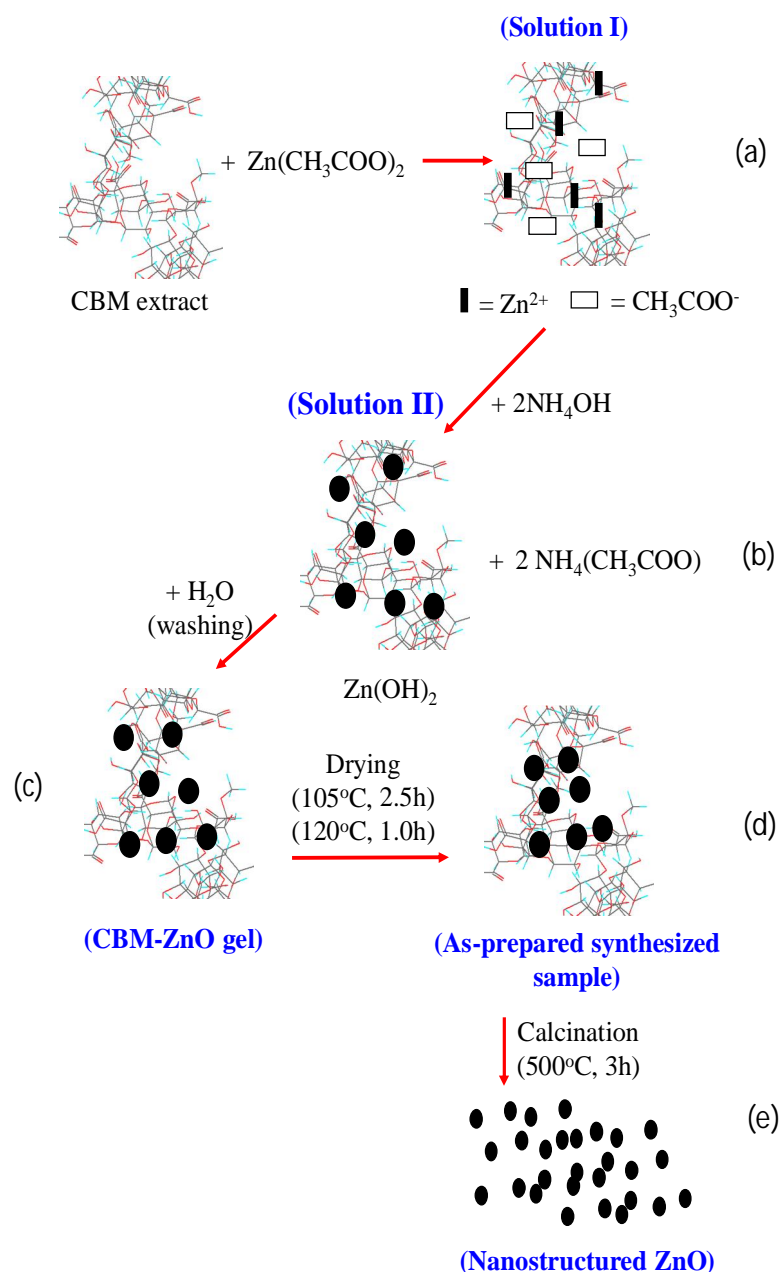


**Fig. 7.** The overall reaction mechanism responsible to form the nanostructured ZnO

removal of the adsorbate from the adsorbent surface may lead to adsorbent deactivation, which suffers its activity. Therefore, the reusability of the nanostructured ZnO is under consideration. To reuse the adsorbent, the nanostructured ZnO particles were heat treated at  $400^\circ\text{C}$  for 2 h. A complete removal of the CR dye molecules from the nanostructured ZnO was confirmed by changing the color of powdered particle from red (Fig. 9a) to yellowish powder

(Fig. 9b). In this study, five experimental cycles were conducted under the same experimental conditions and the results are presented in Fig. 9c. As can be seen from Fig. 9c, from the first to the fifth cycle, a markedly stable activity of the nanostructured ZnO is observed. This result indicates that heat treatment of the nanostructured ZnO is quite suitable to remove the CR dye molecules from the surface. The heat treatment of the reused

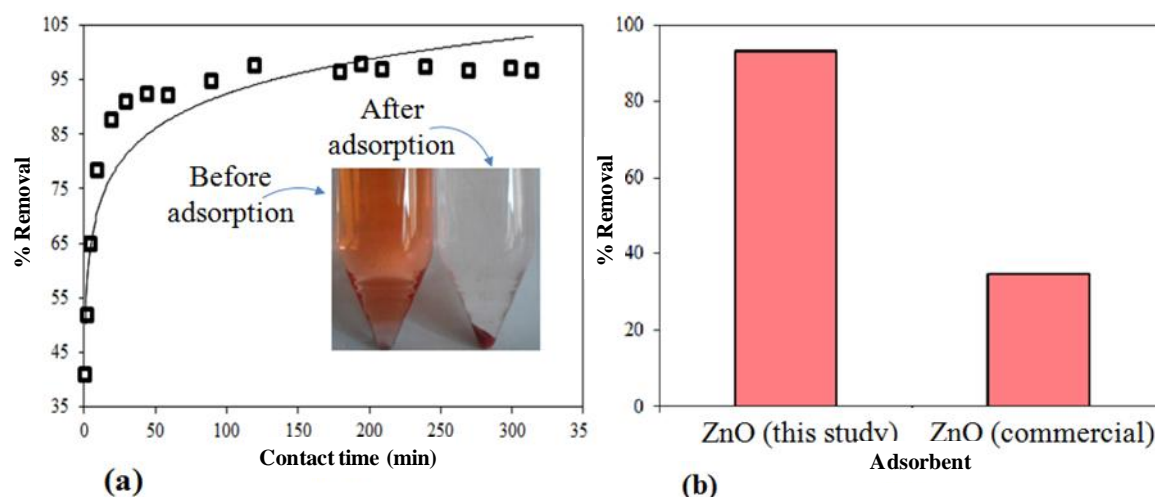


**Fig. 8.** The effect of contact time (min) on the CR dye removal percentage by nanostructured ZnO (a), and comparative removal of CR dye using the synthesized nanostructured ZnO and commercial ZnO (b). (For interpretation of the references to color in this figure the reader is referred to the web version of the article.)

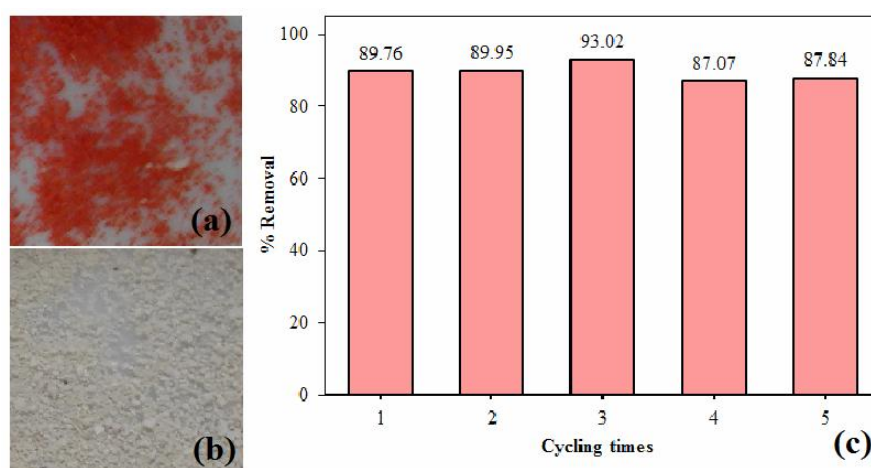


**Fig. 9.** Images of used nanostructured ZnO powder: before heating treatment (a) where the color (red) of the powder was originated from the CR dye molecule attached onto the surface of nanostructured ZnO, after heating treatment in a box furnace at 400 °C for 2 h in open air (b), and the percentage removal of CR dye from five cycles testing using nanostructured ZnO (c). (For interpretation of the references to color in this figure the reader is referred to the web version of the article.)

adsorbent may only remove the CR dye molecules from the adsorbent surface, but it did not significantly alter the adsorbent characteristics, because the treatment process of the reused adsorbent was receiving a significant lower temperature (i.e., 400 °C) than the calcination temperature in the synthesis process of the nanostructured ZnO (i.e., 500 °C). Hence, the activity of the nanostructured ZnO has been continuously well maintained.

#### 4. Conclusion

Nanostructured ZnO was successfully synthesized

by bio-templating method using an extract of the *Cyclea barbata Miers* leaves. The synthesized nanostructured ZnO has a well-defined spherical morphology and good crystalline nature with hexagonal wurtzite structure and space group of P63mc. The synthesized nanostructured ZnO was tested for its potential use as an adsorbent for CR dye removal from water through batch adsorption process. The nanostructured ZnO can rapidly adsorb the CR dye and its performance was found to be higher than the commercial ZnO. In addition, the cycling experiment test showed

that the nanostructured ZnO is markedly stable and its activity was kept continuously maintained after being used for several times. The result of this study indicates that nanostructured ZnO is a promising adsorbent material for the removal of synthetic dyes from aqueous solution. However, more detailed study to understand the environmental effects (adsorbent dose, temperature, pH, ionic strength, dye concentration, etc.) on the removal behavior of the nanostructured ZnO, as well as the kinetic investigations are also interesting to be done.

### Acknowledgements

Mrs. Yulianti Sampora, RCCChem-LIPI is greatly appreciated for helping the FTIR analysis. The authors are very much thankful to anonymous reviewers for their valuable comments, which helped the authors to improve the manuscript.

### References

1. S. Shao, K. Zheng, K. Zidek, P. Chabera, T. Pullerits, F. Zhang, "Optimizing ZnO nanoparticle surface for bulk heterojunction hybrid solar cells", *Sol Energ. Mat. Sol. C.*, Vol. 118, 2013, pp. 43-47.
2. H. Huang, Q. Zhao, K. Hong, Q. Xub, X. Huang, "Optical and electrical properties of N-doped ZnO heterojunction photodiode", *Physica E.*, Vol. 57, 2014, pp. 113-117.
3. M. Bagheri, S. Azizian, B. Jaleh, A. Chehregan. "Adsorption of Cu(II) from aqueous solution by micro-structured ZnO thin films", *Ind. Eng. Chem.*, Vol. 20, 2014, pp. 2439-2446.
4. C. Jayaseelan, A.A. Rahuman, A.V. Kirthi, S. Marimuthu, T. Santhoshkumar, A. Bagavann, K. , L. Karthik, K.V.B. Rao, "Novel microbial route to synthesize ZnO nanoparticles using *Aeromonas hydrophila* and their activity against pathogenic bacteria and fungi", *Spectrochim. Acta A*, Vol. 90, 2012, pp.78-84. <http://dx.doi.org/10.1016/j.saa.2012.1001.1006>
5. K. Ada, A. Ergene, S. Tan, E. Yalçı, "Adsorption of Remazol Brilliant Blue R using ZnO fine powder: Equilibrium, kinetic and thermodynamic modeling studies", *J. Hazard. Mater.*, Vol. 165, 2009, pp. 637-644.
6. Y. W. Baek, Y. J. An, "Microbial toxicity of metal oxide nanoparticles (CuO, NiO, ZnO, and Sb<sub>2</sub>O<sub>3</sub>) to *Escherichia coli*, *Bacillus subtilis*, and *Streptococcus aureus*", *Sci. Total. Env.*, Vol. 409, 2011, pp. 1603-1608.
7. S. Liang, L. Zhu, G. Gai, Y. Yao, J. Huang, X. Ji, X. Zhou, D. Zhang, P. Zhang, "Synthesis of morphology-controlled ZnO microstructures via a microwave-assisted hydrothermal method and their gas-sensing property". *Ultrason. Sonochem.*, Vol. 21, 2014, pp. 1335-1342.
8. C. F. Li, C. Y. Hsu, Y. Y. Li, "NH<sub>3</sub> sensing properties of ZnO thin films prepared via sol-gel method", *Alloys Comp.*, Vol. 606, 2013, pp. 27-31.
9. D. Sahu, B. S. Acharya, A. K. Panda, "Role of Ag ions on the structural evolution of nano ZnO clusters synthesized through ultrasonication and their optical properties", *Ultrason. Sonochem.*, Vol. 18, 2011, pp. 601-607.
10. M. M. Rashad, A. A. Ismail, I. Osama, I. A. Ibrahim, A. H. T. Kandil, "Photocatalytic decomposition of dyes using ZnO doped SnO<sub>2</sub> nanoparticles prepared by solvothermal method", *Arabian J. Chem.*, Vol. 7, 2014, pp. 71-77.
11. M. H. Wang, F. Zhou, B. Zhang, "Surfactant-assisted synthesis of monodispersed ZnO nanorods at low temperature", *Mater. Lett.*, Vol. 114, 2014, pp. 84-87.
12. C. Pholnak, C. Sirisathitkul, S. Suwanboon, D. J. Harding, "Effects of precursor concentration and reaction time on sonochemically synthesized ZnO nanoparticles" *Mater. Res.*, Vol. 17, 2014, pp. 405-411.
13. S. Jiao, K. Zhang, S. Bai, H. Li, S. Gao, H. Li, J. Wang, Q. Yu, F. Guo, L. Zhao, "Controlled morphology evolution of ZnO nanostructures in the electrochemical deposition: From the point of view of chloride ions" *Electrochim. Acta*. Vol 111, 2013, pp. 64-70.
14. H. Zhang, D. Yang, Y. Ji, X. Ma, J. Xu, D. Que, "Low temperature synthesis of flowerlike ZnO nanostructures by cetyltrimethylammonium bromide-assisted hydrothermal process" *J. Physic. Chem. B.*, Vol. 108, 2004, pp. 3955-3958.
15. M. A. Tshabalala, B. F. Dejene, H. C. Swart, "Synthesis and characterization of ZnO nanoparticles using polyethylene glycol (PEG)", *Physica B.*, Vol. 407, 2012, pp. 1668-1671.
16. S. M. Zanetti, A. Andréia da Silva A, "Synthesis and characterization of bismuth zinc niobate pyrochlore nanopowders" *Mater. Res.*, Vol. 10, 2014, pp. 261-266.
17. P. Gu, X. Wang, T. Li, H. Meng, H. Yu, Z. Fan. "Synthesis, characterization and photoluminescence of ZnO spindles by polyvinylpyrrolidone-assisted low-temperature

- wet-chemistry process". *J. Cryst. Growth*. Vol. 338, 2012, pp. 162-165.
18. R. C. Pawar, J. C. Shaikh, A. V. Moholkar, "Surfactant assisted low temperature synthesis of nanocrystalline ZnO and its gas sensing properties". *Sensor Actuat. B.Chem.*, Vol. 151, 2010, pp. 212-218.
  19. J. H. Jang, J. H. Park, H. G. Oh, "Effects of dodecyl sulfate anionic surfactants on the crystal growth of ZnO through hydrothermal process", *J. Ceram. Process. Res.*, Vol. 10, 2009, pp. 783-790.
  20. T. Prakash, R. Jayaprakash, D. S. Raj, S. Kumar, N. Donato, D. Spadaro, G. Neri, "Sensing properties of ZnO nanoparticles synthesized by using albumen as a biotemplate for acetic acid monitoring in aqueous mixture", *Sensors Actuat. B. Chemi.*, Vol. 176, 2013, pp. 560-568.
  21. S. Bitao, W. Ke, D. Na, M. Hongmei, L. Ziqiang, T. Yongchun, B. Jie, "Biomorphic synthesis of long ZnO hollow fibers with porous walls", *J. Mater. Process. Tech.*, Vol. 209, 2008, pp. 4088-4092.
  22. H. F. Greer, W. Zhou, M. H. Liu, Y. H. Tseng, C. Y. Mou, "The origin of ZnO twin crystals in bio-inspired synthesis". *Cryst. Eng. Commun.*, Vol. 14, 2012, pp. 1247-1255.
  23. D. Ramimoghadam, M. Z. B. Hussein, Y. H. Taufiq-Yap, "Synthesis and characterization of ZnO nanostructures using palm olein as biotemplate" *Chem. Central*. Vol. 7, 2013, pp. 71-81.
  24. J. Tam, S. Salgado, M. Miltenburg, V. Maheshwari, "Electrochemical synthesis on single cells as templates", *Chem. Commun.*, Vol. 49, 2013, pp. 8641-8643.
  25. D. Ramimoghadam, M. Z. B. Hussein, Y. H. Taufiq-Yap, "Hydrothermal synthesis of zinc oxide nanoparticles using rice as soft biotemplate", *Chem. Central*. Vol. 7, 2013, pp. 136-146.
  26. P. Atanasova, D. Rothenstein, J. J. Schneider, R. C. Hoffmann, S. Dilfer, S. Eiben, C. Wege, H. Jeske, J. Bill, "Virus-templated synthesis of ZnO nanostructures and formation of field-effect transistors", *Adv. Mater.*, Vol. 23, 2011, pp. 4918-4922.
  27. O. Zuas, H. Abimanyu, W. Wibowo, "Synthesis and characterization of nanostructured CeO<sub>2</sub> with dyes adsorption property", *Proc. Appl. Ceram.*, Vol. 8, 2014, pp. 39-46.
  28. C. Namasivayam, R. Radhika, S. Suba, "Uptake of dyes by a promising locally available agricultural solid waste: Coir pith" *Waste Manage.*, Vol. 21, 2001, pp. 381-387.
  29. Q. L. Sun, L. Z. Yang, "The adsorption of basic dyes from aqueous solution on modified peat-resin particle", *Water Res.*, Vol. 37, 2003, pp. 1535-1544.
  30. M. J. Prival, V. D. Mitchell, "Analysis of a method for testing azo dyes for mutagenic activity in *Salmonella typhimurium* in the presence of flavin mononucleotide and hamster liver S9", *Mutat. Res-Envir. Muta.*, Vol. 97, 1982, pp. 103-116.
  31. S. Ilican, Y. Caglar, M. Caglar, "Preparation and characterization of ZnO thin films deposited by sol-gel spin coating method", *Optoelect. Advanced Mater.*, Vol. 10, 2008, pp. 2578 - 2583.
  32. S. Bagheri, K. G. Chandrappa, S. B. A. Hamid, "Hamid, Facile synthesis of nano-sized ZnO by direct precipitation method" *Der Pharma Chem.*, Vol. 5, 2013, pp. 265-270
  33. L. Xu, B. Wei, W. Liu, H. Zhang, C. Su, J. Che, "Flower-like ZnO-Ag<sub>2</sub>O composites: precipitation synthesis and photocatalytic activity", *Nanoscale Res. Lett.*, Vol. 8, 2013, pp. 536-542.
  34. A. Arkarapanthu, V. Chavasit, P. Sungpuag, L. Phuphathanaphong, "Gel extracted from *Khruea-ma-noi* (*Cyclea barbata* Miers) leaves: chemical composition and gelation properties", *J. Sci. Food. Agri.*, Vol. 85, 2005, pp. 1741-1749.
  35. P. Mackaman, N. Tangsuphoom, V. Chavasit, "Effect of extraction condition on the chemical and emulsifying properties of pectin from *Cyclea barbata* Miers leaves", *Int. Food Res.*, Vol. 21, 2014, pp. 799-806.
  36. R. N. Gayen, K. Sarkar, S. Hussain, R. Bhar, A. K. Pal, "ZnO films prepared by modified sol-gel technique", *Indian J. Pure Appl. Phys.*, Vol. 49, 2011, pp. 470-477.
  37. O. Zuas, H. Budiman, N. Hamim, "Synthesis Of ZnO nanoparticles for microwave induced rapid catalytic decolorization of congo red dye", *Adv. Mater. Lett.*, Vol. 4, 2013, pp. 662-667.
  38. P. B. Balbuena, K. E. Gubbins, "Teoritical interpretation of adsorption behavior of simple fluids in slit pores", *Langmuir*. Vol. 9, 1993, pp. 1801-1814.
  39. U. I. Gaya, A. H. Abdullah, Z. Zainal, M. Z. Hussein, "Photocatalytic degradation of 2,4-dichlorophenol in irradiated aqueous ZnO suspension", *Int. J. Chem.*, Vol. 2, 2010, pp. 180-193.
  40. D. Visinescu, G. Patrinoiu, A. Tirsoaga, O. Carp, *Nanotechnology and Health Risk*, Springer, Netherlands, 2012, pp. 119.

